COBEM 2023 27TH INTERNATIONAL CONGRESS OF MECHANICAL ENGINEERING

ABCM Brazilian Society of Mechanical Sciences and Engineering
27th ABCM International Congress of Mechanical Engineering
December 04-08, 2023, Florianópolis-SC, Brazil

COB-2023-2407
EXPLORING SNAKE-LIKE LOCOMOTION: ANALYSIS OF SERPENOID CURVES AND ANISOTROPIC FRICTION IN SNAKE ROBOTS

Vinicius Carvalho Gomes
Gabriel Baliza Rocha
Mariana Mendanha da Cruz
Thiago de Deus Lima Rocha
Dianne Magalhães Viana
Carla Maria Chagas e Cavalcante Koike
Jones Yudi Mori Alves da Silva
University of Brasília. UnB - Brasília, DF, 70910-900
viniciuscgomes.98@gmail.com ; gabrielbaliza1@gmail.com ; dedeusthiagounb@gmail.com ; mariana.mendanha.mm@gmail.com ; diannemv@unb.br ; carla.koike@gmail.com ; jonesyudi@unb.br

Abstract. *Apodal or snake-like motion is still relatively unexplored in robotics compared to more common forms such as wheels, tracks,and legs. However, locomotion through the robot's own body offers many advantages in scenarios where other common forms of locomotion are not feasible. Due to their flexible and highly adaptive structure, snake robots have an easier time moving in uneven terrains, narrow passages, and overcoming obstacles. The concept of snake robots is often associated with the use of reconfigurable modular robotics. Snakes utilize the anisotropic friction provided by their scales to direct the direction of movement, generating greater friction perpendicular to their body and lower friction parallel to their body. A major challenge in robotics is how to reproduce this behavior provided by the scales in the modules of constructed robots. This study aims to examine the impact of Hirose's serpenoid curve parameters and anisotropic friction on the locomotion of snake robots. To achieve this, simulations and comparisons to similar projects will be conducted, and a module will be used for the modeling of apodal robots, enabling investigations into bioinspired movement. This research contributes to better understand apodal locomotion by investigating the relationship between snake movement and the design parameters of apodal robots. The results highlight the importance of anisotropic friction in achieving serpentine locomotion.*

Keywords: *Modular Robotics, Anisotropic Friction, Simulation, Apodal Robot.*

1. INTRODUCTION

The form of locomotion known as serpentine motion still presents itself as one of the most challenging crawling gaits in robotics compared to more common forms such as wheels, tracks, and even legs. However, self-propulsion using the robot's own body presents many advantages in scenarios where the other more usual forms of locomotion are not feasible, especially when combined with over-actuated robots.

The concept of snake-like robots is often associated with the use of modular robotics. In modular robotics, a robot is composed of a set of M modules that can be reconfigured, allowing the robot to assume different shapes and configurations. The main advantage of modular robotics is its flexibility and versatility. Although snake robots are not commonly applied in traditional, flat surfaces scenarios because of their relative low motion efficiency and payload capacity when compared to other forms of robot locomotion cited above, they are undoubtedly the most versatile group of robots, capable of performing well in a bigger set of scenarios than any other common robots. When analysing their energy consumption while performing in cluttered environments, Liu *et al.* (2021) state that although their redundant actuator structure might consume more power, when the robot traverses these environments, its energy consumption can be comparatively considered low to other types of robots. The current explanation owes to the fact that the snake robots will not consume too much energy in moving different appendages (such as wheels or legs). With their flexible and highly adaptive structure, snake-like robots have an easier time navigating through rough terrain, narrow passages, and overcoming obstacles. For this reason, the applications of snake-like robots are diverse, and there are already studies on the use of these robots in search and rescue operations in debris and hard-to-reach environments (Han *et al.*, 2022), inspection of pipe networks (Selvarajan *et al.*, 2019), and even space exploration missions (Merz *et al.* (2018); Schreiber *et al.* (2020)) .

One of the biggest challenges in constructing a snake-like robot is understanding how friction influences the movement of snakes and designing the robot's modules to mimic the mechanisms used by these animals. Snakes use the anisotropic friction provided by their scales to control the direction of movement, generating higher friction perpendicular to their body and lower friction parallel to their body. A major challenge in robotics, manufacturing sciences and mechanism de-

sign is how to reproduce this behavior provided by scales in the modules of constructed robots. As research in anisotropic surface friction design is an active hotspot, there are some partial solutions proposed.

For example, Serrano *et al.* (2015) propose a fully ridged DC motor actuated modular robot which passively uses its ridges as means to achieve friction anisotropy and therefore perform serpentine locomotion, specially inch-worm gait. However,this model was not capable of performing lateral undulation. Based on real snakes morphology, Galembeck (2018) proposed another passive solution: the use of rigid friction surfaces which could mimic friction anisotropy when placed between the entirety of modules from one snake robot and the ground where it lies on. These structures are easily interchangeable and could be used in any kind of rigid structure modular snake-robot as a way to enhance its friction anisotropy. Although the models proposed take inspiration in real snakes morpholoy, any kind of superficial pattern could have its friction properties tested and validated both in real conditions and simulations. Other solution which relies heavily on manufacturing processes is the one proposed by Lamping *et al.* (2022) which creates a backwards friction coefficient up to 62% higher than its forward component. It is based on the creation of a soft bendable scale like structure with variable geometry at the bottom of the desired module. An older, but also remarkable solution is the one by Marvi *et al.* (2011), which unlike the ones cited above, relies on an active rigid mechanism that is capable of changing the friction coefficients in the same directions as before, however, on static friction, one could reach for backwards friction, even double the value for forward direction friction coefficient.

Another completely different model is presented by Branyan *et al.* (2020). This is a soft robot, pneumatically actuated with polyester plastic sheets as skin cut in japanese Kirigami style with multiple cut patterns. As the robot is actuated, it bends and the cut surface patterns buckle, which changes the robot superficial profile, creating friction anisotropy which is capable of generating the desired lateral undulation gait. To increase lateral superficial resistance, this plastic sheet skin also undergoes microornamentation. Lastly, the work presented by Ta *et al.* (2018) depicts the use of multimaterial 3D printing to create capillary like friction surfaces. In this case, each capillary has a double material cross section. Part of this section is made by a high coefficient of friction and the rest is made by a high coefficient of friction material. By the careful choice of proportion and the correct placement of each structure, it is possible to create surface anisotropy, with desired high lateral friction and low forward friction. All these references show that there are several criteria to choose the best research strategy for creating the best mechanical designs to induce friction anisotropy. By using cost and interchangeability as the major decision criterion, we chose to test the solution by Galembeck (2018).

In addition to friction, another important factor for the movement of a snake-like robot is its movement curve and motion control or gait generation strategy. In the field of bioinspired robotics, a common practice to generate rhythmic motor patterns is the use of the Central Pattern Generator (CPG) approach. As an example,Li *et al.* (2015) used it to generate asymetric oscilations to move a snake-like robot with caterpillar-like rectilinear undulation movement through controlled terrain. Marvi *et al.* (2019) used it to optimize, by simulation,the terrain traversal of a snake robot by using a reference tracking framework known as integral Line-of-sight (LOS) controller. Another similar strategy was adopted by Cao *et al.* (2022), using CPGs and the adaptative Line-of-sight (LOS) controller. According to Gómez (2008), if locomotion is to be studied at the permanent regime, CPGs could be replaced by simpler, but effective sinusoidal generators.

Shigeo Hirose proposed a mathematical description for the shape of a snake's body during its movement based on his studies with snakes in Hirose and Yamada (2009). This description is still widely used, both for continuous and discrete models today in the implementation of serpentine robots and is known as a serpenoid curve, due to its resemblance to a sine wave. In order to better understand Hirose's curve, it is necessary to define its terms: The parameter s stands for the robot's distance relative to its tail along its own body. From head to tail, it determines the entire modular robot's length l. α_s stands for the serpenoid curve inclination at robot's length s; $\alpha = a = A$, the winding angle, which is also α_s at $s = 0$. Figure (1a) shows the theoretical effect of a in Hirose's serpenoid curve and Fig. (1b) depicts its maximum value so that its modules do not collide. k determines the robot's number of undulations. Each robot is made by M modules. Figure (1f) shows that the greater the number of modules, the better the similarity between discrete and continuous model for serpenoid curve. Each module can have partial lengths d_0 and d, measured between each links extremity and the center of the module's joint. Parameter $B = b = 2\pi k$ encapsulates the effect of parameter k which can be seen on Fig.(1c). Parameter $c = C$ determines an offset which rotates the orientation of the snake robot's trajectory. The orientation of the module can be defined by a vector $\mathbf{o}$ and the offset c causes the orientation vector and the x axis of locomotion to form an angle. Figure (1d) shows the theoretical effect of c in the robot's curve of locomotion. Equation (1) defines the curvature of Hirose's curve, which is also the inclination of any line tangent to the curve at a point s.

$$\alpha_s = \alpha \cdot cos\Big(\frac{2\pi k}{l}\Big). \tag{1}$$

Equations (2) and (3) present how a robot's point position can be calculated along its length s, as defined in Hirose and Yamada (2009). However, the procedure described by these equations is not analitically achievable, then it is necessary to numerically integrate these variables so as to gather useful information about the robot's position. In order to effectively perform these calculations and better understand how a continuous model can be used to describe a discrete modular robot, it is important to recall that the serpenoid curve is discretized by using a M module sequential array of interconnected

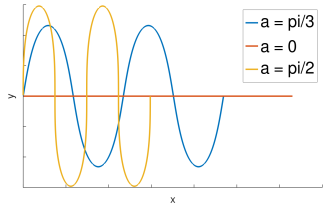

(a) Parameter A influency on the curve.

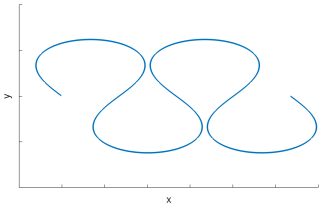

(b) Parameter A max value : $A = 120°$.

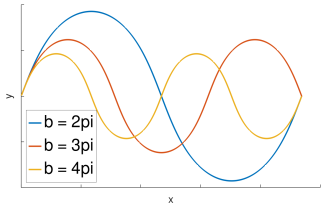

(c) Parameter B influency on the curve.

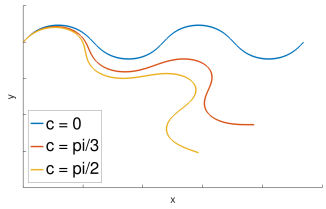

(d) Parameter C influency on the curve.

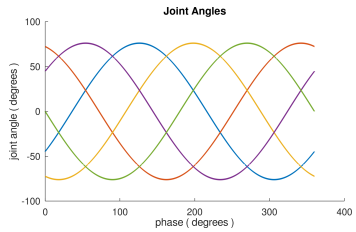

(e) Joint angles over time for 5 modules robot.

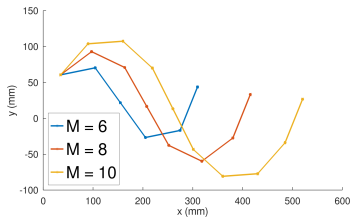

(f) Discrete serpenoid curve for M = 6, M = 8 and M = 10.

Figure 1: Basic serpenoid curve parameters visual influence.

block's(both links and joints) which can move relative to each other more commonly via relative rotation. By controlling the joint angles between each of the module's links, the serpenoid curve can be mimetized. Each motion control method differs by the way that they controle these angles. The higher the number of modules, the better the approximation between the discrete and continuous serpenoid curve.

$$x(s) = \int_0^s \cos(\alpha_s) ds, \tag{2}$$

$$y(s) = \int_0^s \sin(\alpha_s) ds. \tag{3}$$

For a module which has equal partial module lengths $d_0 = d$, the respective joint angle equation becomes Eq. (4), as demonstrated by Gómez (2008).

$$\phi_i(t) = -2 \cdot a \cdot \sin\left(\left(\frac{b}{2 \cdot M}\right) \cdot \sin\left(wt + \left(\frac{i \cdot b}{M}\right)\right) - \frac{c}{M}\right). \tag{4}$$

Because Eq. (2) and Eq. (3) do not have a closed form solution, they have to be numerically calculated by the discrete equations. One of the possible solutions to this problem was proposed by Qiao *et al.* (2017). This solution is represented in Eq. (5) and Eq. (6). By considering each module as a rigid structure, one can determine the position of any point of the robot by using these equations, which means that the robot kynematics could be calculated at will.

$$x_i = \sum_{k=1}^{i} \frac{1}{M} \cos\left(a \cdot \cos\left(\frac{kb}{M}\right) + \left(\frac{kc}{M}\right)\right), \tag{5}$$

$$y_i = \sum_{k=1}^{i} \frac{1}{M} \sin\left(a \cdot \cos\left(\frac{kb}{M}\right) + \left(\frac{kc}{M}\right)\right). \tag{6}$$

So as to increase the knoweledge about the effect of parameter change in control models relative to the modular robot's trajectory, the present article aims to simulate the movement of a modular snake robot in different parameter scenarios and analyze how each of the variable parameters affects the robot's trajectory and velocity. The parameters tested will contain both virtual control parameters and also phisical quantities like friction coefficients. At the end of the article,we expect to gather data to get closer to answering the non-trivial question: "How low should forward friction and how high should orthogonal friction be in order for a snake robot to move?" All these tests will serve as both control and design guidelines for future modular snake robots with similar configurations.

2. METHODOLOGY

2.1 Proposed Module

In order to perform the locomotion, Galembeck (2018) proposes a new module: VDM-Y in Fig.2a, which is perfected in Rocha (2023) and later manufactured with a Creality FDM Ender-3 V2 3D printer using Polylactic acid (PLA) plastic filament. Its design was based on 3 main principles: Its inferior surface must be able to attach to interchangeable friction surfaces; each module must be able to move at least other 2 yaw modules;the module must be as simple as possible in order to perform the yaw-yaw desired movement.

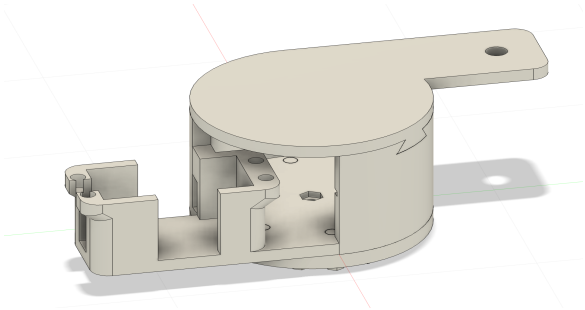

(a) New VDM-Y module.

(b) Real 3D printed VDM-Y module. Source: Rocha (2023).

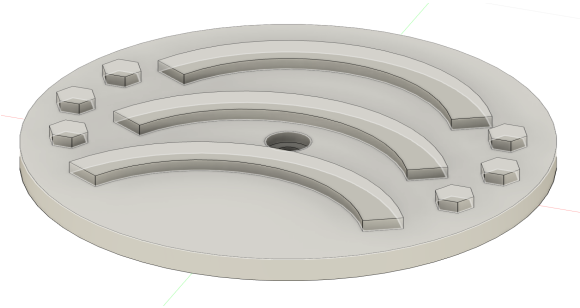

(c) first geometry for friction surface.

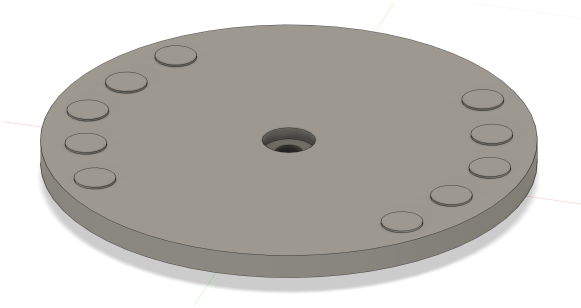

(d) second geometry for friction surface.

Figure 2: VDM-Y module's components and assembly.

Within each module there is an Arduino microcontroller, a MG955 servomotor, external batteries and wiring both for power supply and module comunication. The module's mechanical properties are all calculated via SolidWorks. Each module full assembly weights 100.78 g, which is 10% of the module mass in Baysal and Altas (2020) and 67% of the module mass in Li *et al.* (2015). Each motor has a torque of 0.92 N.m, which is roughly 3 times higher than the torque used in Li *et al.* (2015). By using 0.19 m as the distance between joint axis,there is more than enough motion capacity to move 2 other modules at maximum friction conditions. On the other hand, the distance between axis used in Li *et al.* (2015) is 76 mm which reduces the torques on the motors. However, by using a higher axis distance, the proposed module is capable of receiving aditional embedded devices such as sensors and other controllers within its cilindrical encasing. The idea of using interchangeable friction surfaces to test its direction anisotropy presents many advantages, especially in terms of low manufacturing cost and low residue waste. Figures 2c and 2d show different friction surfaces which will be used in further testing.

2.2 Simulator and Simulation Configurations

There is a growing number of robotics simulators available for use, such as Gazebo, V-REP/CoppeliaSim, Simulink. The decision on which one to use will depend on a variety of factors, such as: use of friction anisotropy, physics engine implemented, robustness of mathematical calculations, capability of importing external pieces and scenarios, purchase cost and others. To simulate a wheeled robot with adaptative path following algorithms, Cao *et al.* (2022)and Marvi *et al.* (2019) used V-REP with Bullet physics engine, with aid from Matlab and Open Dynamics Engine (ODE). To simulate caterpillar-like gaits, Li *et al.* (2015) used ODE and later compared its results with real sampled data. To simulate the effects of different ratios of friction anisotropy for a wheel-less robot, Baysal and Altas (2020) used Matlab/Simulink, however its modelling was only possible because the module it used had ideal and user configurable friction properties. To the best of our knowledge, one of the only graphical simulation software which is capable of both showing simulation images and performing complex physical calculations is Gazebo.

So as to to set up the simulation, the Gazebo simulation software is chosen. It uses ODE(Open Dynamics Engine) to

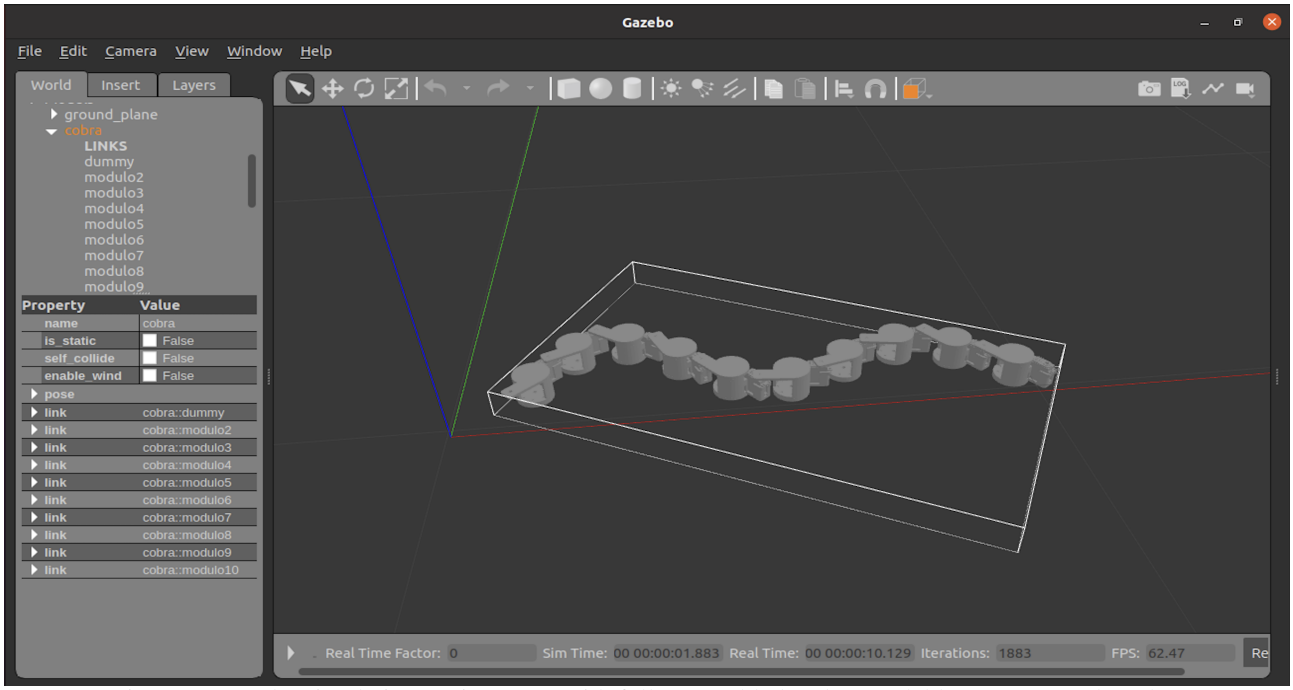

Figure 3: Gazebo simulation environment with fully assembled and controlable VDM-Y snake robot

simulate the robot's locomotion and allows the use of anisotropic friction between surfaces through the use of a «gazebo>" element. This element contains 3 configurable parameters: μ_1, μ_2 and $\mathbf{fdir1}$. μ_1 and μ_2 are friction coefficients related to orthogonal directions. $\mathbf{fdir1}$ is a basis vector which indicates the direction for μ_1. Through the use of Gazebo's "SW2URDF" extension it was possible to import the fully functional URDF 10 module snake robot file from its original assembly file on SolidWorks. Therefore, no simplification of the module's design was required, which leads to a better trustworthiness of the simulated results compared to real scenario cases. The robot's joint control is done by ROS (Robot Operating System). Within its environment, a fully proportional controller is used to act on each joint of the robot. For a specific set of PID parameters, the fully proportional controller showed the best results regarding desired rise time and overshoot, therefore it will be used as the default setup for joint locomotion throughout the entire simulation.

To calculate the robot's position, the first module(the robot's "head") was used as a reference. Its position was numerically calculated by Eq. (5) and Eq.(6) and an ideal scenario of anisotropic friction was considered. Figure (3) depicts the entire modular robot simulation, as well as one of ts possible geometrical configurations during its locomotion.

This article aims to study how each of the parameters A, B, C, the friction anisotropy and the geometrical effect of friction surfaces affect the robot's trajectory and velocity and also compare their effect to solutions presented by (Cao *et al.* (2022); Baysal and Altas (2020); Li *et al.* (2015); Marvi *et al.* (2019)). For each test, only one of the parameters will be alteredwhile the rest remain constant. This approach is expected to guarantee the accuracy and reliability of the results, facilitating a comprehensive understanding of the individual impact of each parameter under investigation.

As a starting point, the curve parameters were randomly set and for each set of parameters, the position of the head was calculated as a function of time, friction coefficients were set to maximum anisotropy, which stands for a high lateral friction coefficient and a low linear friction coefficient throughout the entire simulation. Besides the linear displacement parallel to the robot's body, there was always a lateral displacement perpendicular to the robot's body. It was conjectured that this lateral displacement was present due to the asymmetry of the module which is believed to create a resultant force in favor of the rotation of the robot.

2.3 Parameter C

In Hirose's curve, parameter C is a offset value used to rotate the curve's axis, altering its direction. It was expected that by using parameter C, it would be possible to compensate for the lateral displacement observed in the robot's movement.

So as to test this hypothesis, simulations were conducted using the arbitrary constant set of parameters $A = 0.4\pi$, $B = 4\pi$, $\mu_1 = 0$, $\mu_2 = 0.9$ and $\mathbf{fdir1} = [1, 0, 0]$ and a variable parameter C value. As C varies, it will be possible to observe how it affects the trajectory of the snake robot both laterally and linearly.

2.4 Parameter B

Theoretically, B determines how many periods will occur in the serpenoid curve at any time. In order to analise the effect of B in the robot's movement, simulations were conducted using the constant set of parameters from the previous simulation with the least lateral displacement. Such parameters are $A = 0.4\pi$, $C = \frac{\pi}{6}$, $\mu_1 = 0$, $\mu_2 = 0.9$ and $\mathbf{fdir1} = [1, 0, 0]$. B is a variable parameter. How it varies from 2π to 4π will enlighten the understanding on its effects on the trajectory of the snake robot both laterally and linearly.

2.5 Parameter A

In Hirose's curve, Parameter A influences the curvature of the curve, meaning that a higher A value represents tighter curves and larger steering angles. The parameters were chosen based on the result with the highest linear displacement observed in the test shown in Figure 5a. Such parameters are $B = 3\pi$, $C = \frac{\pi}{6}$, $\mu_1 = 0$, $\mu_2 = 0.9$ and $\mathbf{fdir1} = [1, 0, 0]$ all constant. A varies from $\frac{2\pi}{5}$ to $\frac{2\pi}{7}$ and its influence on the module's linear displacement is measured.

2.6 Influence of anisotropy on linear displacement

It is known that in order for a apodal robot to move, there must be anisotropy between friction coefficients of the lateral and linear directions (Liljebäck *et al.*, 2013). However, the difference between these coefficients in order to establish effective locomotion is not thoroughly known. So as to better understand these relations of friction anisotropy between μ_1 and μ_2, simulations were set with the following parameters: $A = \frac{2\pi}{6}$, $B = 3\pi$, $C = \frac{\pi}{6}$ and $\mathbf{fdir1} = [1, 0, 0]$. The first tests sets μ_1 to a low value, close to 0 Then, μ_2 gradually decreases from a high, close to 1, to a low value and its influence on the linear displacement is measured. The second test sets μ_2 to a high constant value. Then, μ_1 varies from a low to a high value, which corresponds to an increase in the linear direction friction coefficient. Analogously, its effect on the trajectory and velocity is measured within its range of variation. The majority of low cost everyday materials will have its friction coefficients constrained in the range $\mu \in [0, 1]$, so it makes sense to simulate within this range. However, one could simulate with rubber like materials, as done by Baysal and Altas (2020), ranging beyond $\mu = 1$.

Within the simulation it is possible to set isotropic friction coefficients and , by inserting the robot with surfaces 2c and 2d see if their geometry is capable of generating anisotropic friction throughout the locomotion. The simulation time is initially set to 10s and the parameters are the same as before. There are 2 different friction surfaces being tested, therefore, two tests will be performed exactly the same way, except for the surface geometries.

3. RESULTS

3.1 Parameter C

Within the range $C \in [0, \frac{\pi}{4}]$ defined in Fig. 4a, it can be observed that although it is possible to control the direction of movement using parameter C, as also shown in Baysal and Altas (2020), there was not a fixed parameter C that completely eliminated lateral displacement. As observed in Figure 4b, linear displacement is only affected when the robot undergoes rotation due to lateral movement. This graphic pattern is similar to the one presented by Li *et al.* (2015). In other words, displacement in the direction parallel to the robot's body remains unchanged with variations in parameter C.

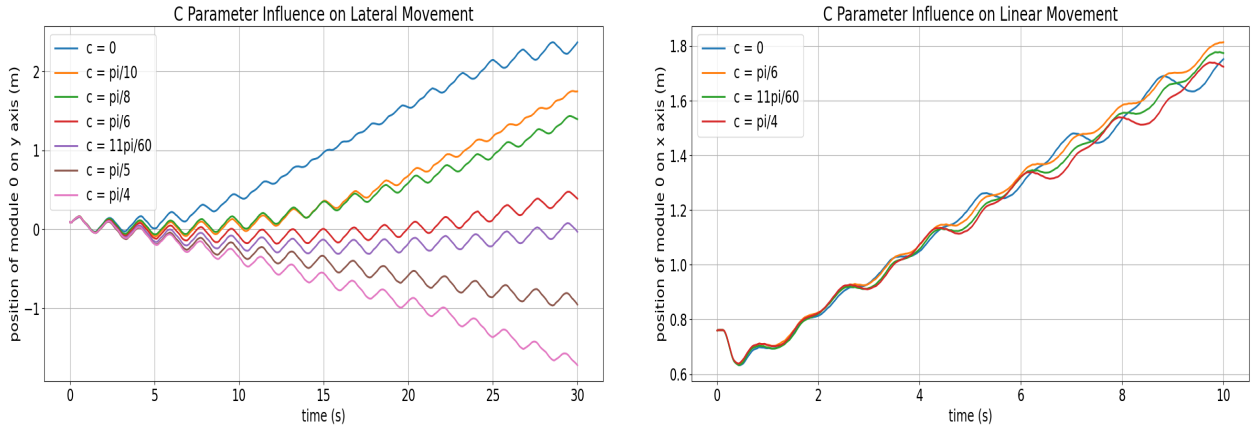

(a) Influence of parameter C on lateral displacement. (b) Influence of parameter C on linear displacement.

Figure 4: Influence of parameter C on linear and lateral displacement.

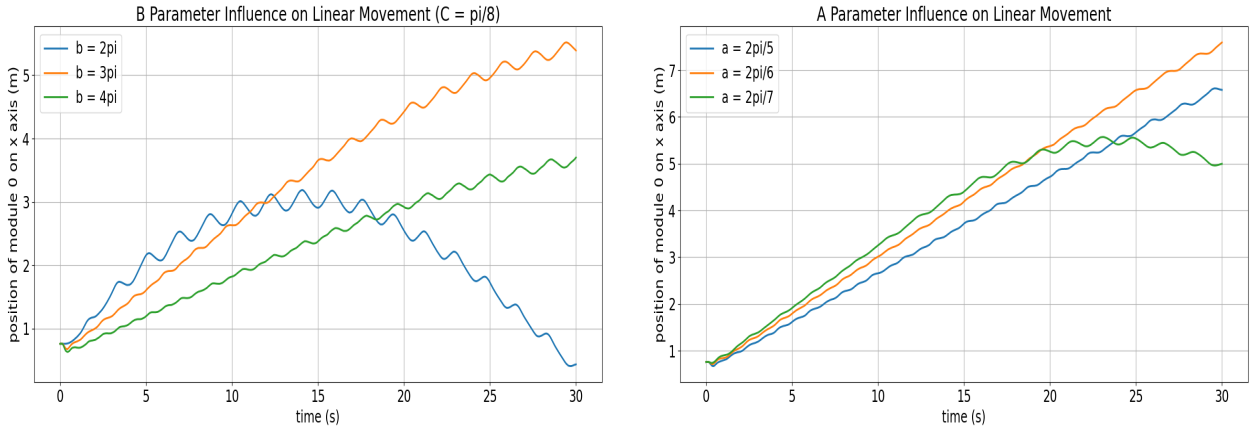

(a) Parameter B influency on linear displacement. $C = 22.5°$.

(b) Parameter A influency on linear displacement.

Figure 5: Influence of parameters A and B on linear displacement.

3.2 Parameter B

The variation of B within the range of $[2\pi, 4\pi]$ has shown that it is inversely proportional to the linear displacement . For a different value constant C value of $\frac{\pi}{8}$, it can be seen in Fig 5a on one hand,that the greater the B value, the less lateral displacement and the smaller the tendency of rotation throughout the locomotion. On the other hand, a smaller B value is more useful to shift the robot's orientation and direction of movement, also because of its greater tendency to rotate and its greater lateral displacement in short periods of time.

3.3 Parameter A

Figure 5b displays the robot's head linear displacement over time as a parametric function of Parameter A. It can be seen that analogously to parameter B, A is inversely proportional to the linear displacement of the robot. However, the robot's trajectory is more sensitive to changes in A in terms of trajectory drifts, specifically a quicker rotation of the module.

3.4 Influence of anisotropy on linear displacement and velocity

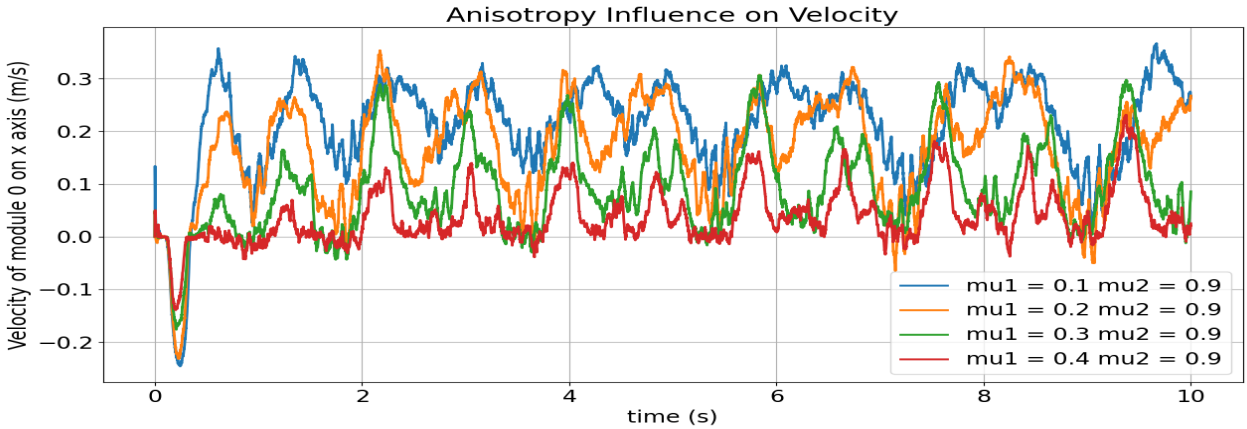

Figure 6: Friction anisotropy influence on linear velocity

For the first test in Fig. 7a the decrease in μ_2 shows that, even for low anisotropy differences (0.1 between directions) the robot is able to move in the linear plane of locomotion. However, for isotropic friction conditions : $\mu_1 = \mu_2$, the robot is unable to displace itself, which is different from the case presented by Baysal and Altas (2020) where a low forward velocity could still be observed. The second test results in Fig. 7b show that the more μ_1 increases by steps of 0.1, the more unable the robot is to displace itself. Relatively to the first test, the variation of μ_1 mantaining a high μ_2 acts faster in order to stop the robot's locomotion. Also, there is a smaller gap for values which enable the robot's locomotion, because, in the second case, even for friction coefficients differences of up to 0.4 ($\mu_1 = 0.5$ and $\mu_2 = 0.9$), there was no

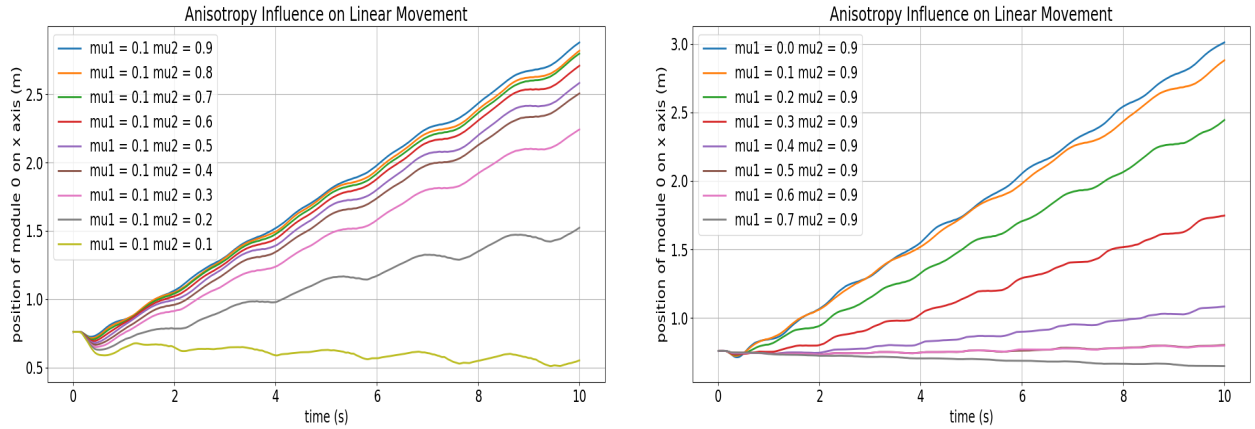

(a) Friction anisotropy influence on linear displacement for μ_1 constant and low.

(b) Friction anisotropy influence on linear displacement for μ_2 constant and high.

Figure 7: Friction anisotropy influence on linear displacement.

visible linear displacement. These results display an important information within the range $\mu \in [0, 1]$: although a high anisotropy is necessary and desired in apodal robots locomotion, it is also highly important that the friction coefficient relative to the linear locomotion be as low as possible, which, as Fig.6 depicts also increases the linear velocity. In this scenario, if it comes to choosing between low anisotropy with a low μ_1 or a higher anisotropy with a high μ_1, the first one should be selected. However, if higher friction coefficients are considered, both linear displacement and velocity can be dramatically increased by keeping $\mu_1 = 1$ and varying μ_2 up to 5, which is achievable for rubber-like materials. Figure 6 is very similar to the velocity profiles shown in (Baysal and Altas (2020); Li *et al.* (2015)). Quantitatively, however, the case studied can reach velocities up to almost 18 times the one shown in Baysal and Altas (2020) and up to almost 10 times the one presented by Li *et al.* (2015).

Aiming to study the geometrical induction of friction anisotropy by using two different friction surfaces in Fig. 2c and 2d these two surfaces were tested during a locomotion test. Neither of these geometries were able to effectively induce friction anisotropy throughout the tests, because there was no displacement of the apodal robot. For the first test, Figure 8a might lead the reader to believe that there was an effective displacement of the robot, however, for a larger span of time, such as 30s in Fig. 8b it is possible to visualize that the robot only rotates and reaches its same initial position, therefore not performing any useful displacement.

The second test using the second geometry surface also has the same results. Figure 9a might lead the reader to think that there was any displacement whatsoever, but even for $\mu = 0.1$, which apparently caused the greater "displacement", if a larger span of time is analized, such as in Fig 9b, it is also clear that no real displacement has occured.

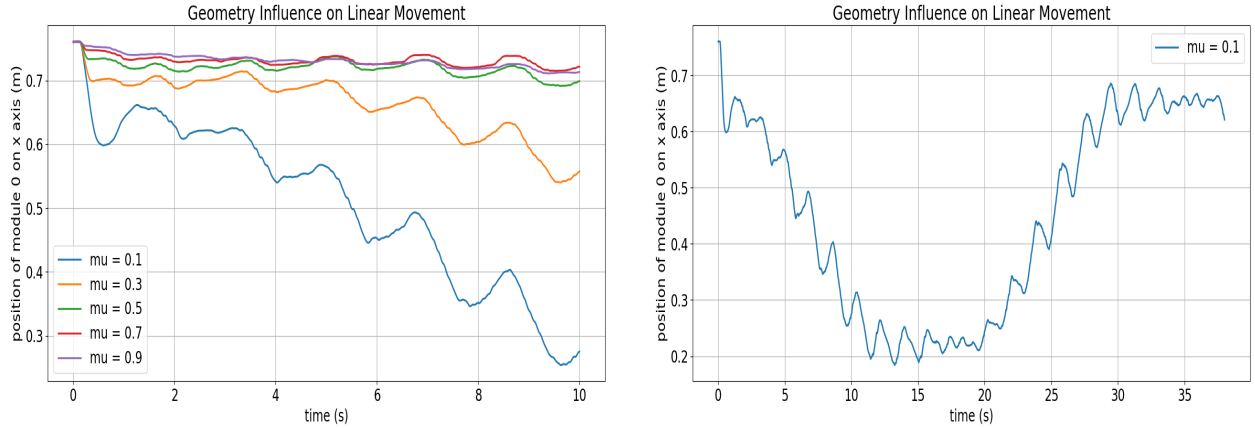

(a) Observed linear displacement using the first friction surface.

(b) Full cycle of rotation for $\mu = 0.1$ using first friction surface .

Figure 8: First friction surface's influence on robot's locomotion.

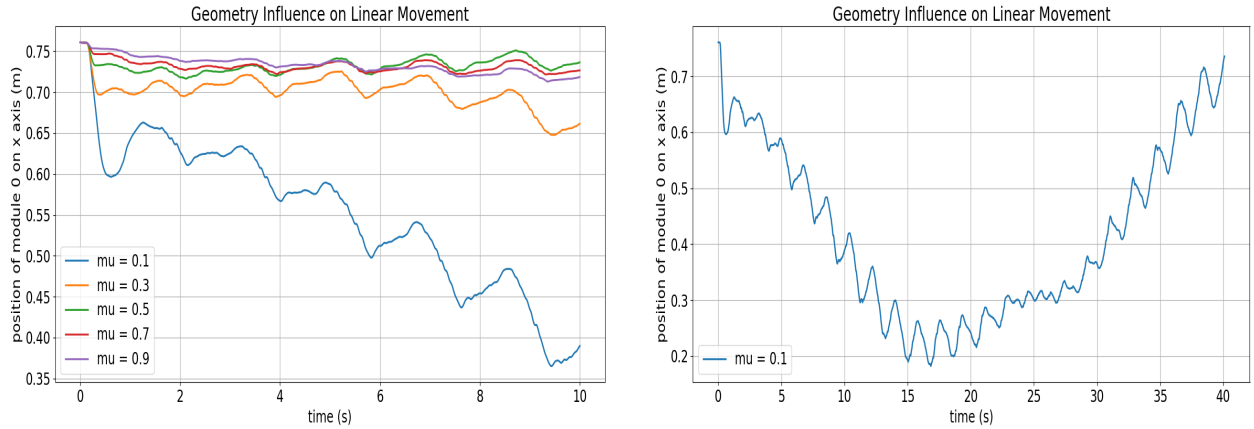

(a) Observed linear displacement using the second friction surface.

(b) Full cycle of rotation for $\mu = 0.1$ using second friction surface.

Figure 9: Second friction surface's influence on robot's locomotion.

4. CONCLUSIONS

This article presents one of many locomotion gaits performed by snake robots and explores how the trajectory of the robot changes as each parameter of Hirose's curve changes. A new yaw-yaw module has been proposed to perform movement over the 2D horizontal plane and through simulations on Gazebo, this new module's trajectory was analyzed likewise.

The results presented enlightened the understanding of how to control the robot's trajectory, direction, velocity and displacement stabilty through the variation of parameters of its motion control serpenoid curve. Each robot has a unique set of specifications, such as number of modules, maximum motor torque and velocity and maximum joint angle. This set of specifications can be used to determine the optimal set of serpenoid curve parameters in order to better perform the intended task.

In order to effectively move via serpentine locomotion, snake robots necessarily need surface friction anisotropy. Section (3.4) shows that displacement cannot occur unless there is friction anisitropy, which proves Hu *et al.* (2008) were right. When the range $\mu \in [0, 1]$ is considered, the importance of keeping a low friction coefficient μ_1 parallel to the robot's body even when the overall anisotropy decreases has been highlighted. However, based on the results from Baysal and Altas (2020), it is also of utmost relevance that a further study on friction coefficient ratios $\frac{\mu_1}{\mu_2}$ for a range $\mu \in [0, \gamma]$, $\gamma \geq 1$, is conducted. Tests executed in section (3.4) proved that these geometrial surfaces did not generate enough friction anisotropy in order to move the robot.

Because of the fact that not enough friction anisotropy has been achieved with the proposed solid material surfaces and only yaw-yaw movement was adopted throughout the experiments, future work could focus on developing soft material surfaces, like those described by Serrano *et al.* (2015),Branyan *et al.* (2020) or Ta *et al.* (2018),which could better induce friction anisotropy and comply to the terrain specific characteristics. By using different modules and different module's connections, other locomotion gaits could be performed and analized similarly.

5. ACKNOWLEDGEMENTS

We would like to express our sincere gratitude to the Mechanical Engineering Department and The Faculty of Technology of University of Brasília for their material and institutional support, which has played a crucial role in the successful completion of this article.

6. REFERENCES

Baysal, Y.A. and Altas, I.H., 2020. "Modelling and simulation of a wheel-less snake robot". In *2020 7th International Conference on Electrical and Electronics Engineering (ICEEE)*. pp. 285–289. doi: 10.1109/ICEEE49618.2020.9102599.

Branyan, C., Hatton, R.L. and Mengüç, Y., 2020. "Snake-inspired kirigami skin for lateral undulation of a soft snake robot". *IEEE Robotics and Automation Letters*, Vol. 5, No. 2, pp. 1728–1733. doi:10.1109/LRA.2020.2969949.

Cao, Z., Zhang, D. and Zhou, M., 2022. "Direction control and adaptive path following of 3-d snake-like robot motion". *IEEE Transactions on Cybernetics*, Vol. 52, No. 10, pp. 10980–10987. doi:10.1109/TCYB.2021.3055519.

Galembeck, T.F., 2018. "Processo para medicao e avaliacao de atrito com fins de facilitar movimentacao de robo apode".

Gómez, J.G., 2008. *Modular Robotics and Locomotion: Application to Limbless Robots*. Ph.D. thesis.

Han, S., Chon, S., Kim, J., Seo, J., Shin, D.G., Park, S., Kim, J.T., Kim, J., Jin, M. and Cho, J., 2022. "Snake robot gripper module for search and rescue in narrow spaces". *IEEE Robotics and Automation Letters*, Vol. 7, No. 2, pp. 1667–1673. doi:10.1109/LRA.2022.3140812.

Hirose, S. and Yamada, H., 2009. "Snake-like robots [tutorial]". *IEEE Robotics Automation Magazine*, Vol. 16, No. 1, pp. 88–98. doi:10.1109/MRA.2009.932130.

Hu, D.L., Nirodya, J., Scotta, T. and Shelleya, M.J., 2008. "The mechanics of slithering locomotion".

Lamping, F., Gorb, S.N. and de Payrebrune, K.M., 2022. "Frictional properties of a novel artificial snakeskin for soft robotics". *Biotribology*, Vol. 30, p. 100210. ISSN 2352-5738. doi:https://doi.org/10.1016/j.biotri.2022.100210.

Li, G., Li, W., Zhang, J. and Zhang, H., 2015. "Analysis and design of asymmetric oscillation for caterpillar-like locomotion". *Journal of Bionic Engineering*, Vol. 12, No. 2, pp. 190–203. ISSN 1672-6529. doi: https://doi.org/10.1016/S1672-6529(14)60112-8.

Liljebäck, P., Pettersen, K., Stavdahl, and Gravdahl, J., 2013. *Snake Robots: Modelling, Mechatronics, and Control*. ISBN 978-1-4471-2995-0. doi:10.1007/978-1-4471-2996-7.

Liu, J., Tong, Y. and Liu, J., 2021. "Review of snake robots in constrained environments". *Robotics and Autonomous Systems*, Vol. 141, p. 103785. ISSN 0921-8890. doi:https://doi.org/10.1016/j.robot.2021.103785.

Marvi, H., Meyers, G., Russell, G. and Hu, D.L., 2011. "Scalybot: A Snake-Inspired Robot With Active Control of Friction". *ASME 2011 Dynamic Systems and Control Conference and Bath/ASME Symposium on Fluid Power and Motion Control, Volume 2*. doi:10.1115/DSCC2011-6174.

Marvi, H., Meyers, G., Russell, G. and Hu, D.L., 2019. "Adaptive Path Following and Locomotion Optimization of Snake-Like Robot Controlled by the Central Pattern Generator". *Hindawi Complexity, Volume 2019*. doi: 10.1155/2019/8030374.

Merz, M., Transeth, A.A., Johansen, G. and Bjerkeng, M., 2018. "Snake robots for space applications".

Qiao, G., Wen, X., Lin, J., Wang, D. and Wei, Z., 2017. "Sigmoid transition approach of the central pattern generator-based controller for the snake-like robot". *International Journal of Advanced Robotic Systems*.

Rocha, G.B., 2023. "Análise experimental de aspectos de comunicação, construção e atrito de robô Ápode bioinspirado".

Schreiber, D.A., Richter, F., Bilan, A., Gavrilov, P.V., Man Lam, H., Price, C.H., Carpenter, K.C. and Yip, M.C., 2020. "Arcsnake: An archimedes' screw-propelled, reconfigurable serpentine robot for complex environments". In *2020 IEEE International Conference on Robotics and Automation (ICRA)*. pp. 7029–7034. doi: 10.1109/ICRA40945.2020.9196968.

Selvarajan, A., Kumar, A., Sethu, D. and bin Ramlan, M.A., 2019. "Design and development of a snake-robot for pipeline inspection". In *2019 IEEE Student Conference on Research and Development (SCOReD)*. pp. 237–242. doi:10.1109/SCORED.2019.8896254.

Serrano, M.M., Chang, A.H., Zhang, G. and Vela, P.A., 2015. "Incorporating frictional anisotropy in the design of a robotic snake through the exploitation of scales". In *2015 IEEE International Conference on Robotics and Automation (ICRA)*. pp. 3729–3734. doi:10.1109/ICRA.2015.7139717.

Ta, T.D., Umedachi, T. and Kawahara, Y., 2018. "Design of frictional 2d-anisotropy surface for wriggle locomotion of printable soft-bodied robots". In *2018 IEEE International Conference on Robotics and Automation (ICRA)*. pp. 6779–6785. doi:10.1109/ICRA.2018.8463177.

7. RESPONSIBILITY NOTICE

The authors are solely responsible for the printed material included in this paper.